Aalto University

Aaltodoc

OPEN ACCESS

Author(s): Roschier, Leif & Hakonen, Pertti J.

Title: Design of cryogenic 700 MHz HEMT amplifier

Year: 2004

Version: Pre-print

Please cite the original version:

Design of Cryogenic 700 MHz HEMT Amplifier

Leif Roschier[*] and Pertti Hakonen

September 16, 2003

Helsinki University of Technology, Low Temperature Laboratory,

Otakaari 3 A, Espoo, FIN-02015 HUT, Finland

Abstract

We present a way to design a high-frequency low-temperature pHEMT-based balanced amplifier. The design is based on measured cryogenic S-parameters combined with a small-signal noise model. Using the design process we constructed an amplifier that was measured to have a gain of 16 dB and a noise temperature of $\sim$ 3 K when cooled to 4.2 K.

[*]Electronic address: `leif.roschier@hut.fi`

I. INTRODUCTION

Quantum information processing in solid state circuits imposes strong requirements on the speed of read-out electronics of qubits as the information is quickly lost due to dephasing. One candidate for fast read-out purposes is the RF-SET [1–3], an amplitude modulated single electron transistor (SET) [4] that is the fastest and the most sensitive electrometer known today. In an usual RF-SET system, the SET is the first-stage amplifier and a high electron mobility transistor (HEMT) works as a second stage amplifier. The noise temperature of the HEMT amplifier should be in the subkelvin range in order to reach the physical limit of the RF-SET, set by the shot-noise of the SET [5]. Technologically, noise temperatures of cryogenic HEMT amplifiers seem to be limited to a few Kelvins [6]. In order to decrease the noise temperature of the amplifiers in the Gigahertz range, DC-SQUID (direct current - superconducting quantum interference device) based amplifiers have been constructed and demonstrated to give subkelvin noise temperatures [7]. However, high frequency SQUID amplifiers are still under development and there are issues related to the input match and stability to be solved before they can be used as general-purpose amplifiers in the GHz range.

First practical cryogenically-cooled GaAs amplifier was demonstrated in 1980 [6, 8]. It took about 9 years after that to develop a working noise model for HEMTs at low temperatures [9]. A good review of the history of HEMT amplifiers and of the design and performance of state-of-the-art amplifiers is found in Ref. [6]. Over the past years, most of the HEMT amplifiers have been designed for the research in radio-astronomy. Today, there is an ever-increasing demand for cryogenic high frequency amplifiers for experiments in the field of condensed-matter physics. RF-SET measurement setup is one example, where low-noise high-frequency amplifiers are needed. In this article we explain the design process of a cryogenic pHEMT (pseudomorphic High Electron Mobility Transistor) based amplifier, e.g. for RF-SET measurement configuration. We used cryogenic measurement data in conjunction with the Pospiezalski noise model [9] to build an amplifier that shows a noise temperature of ~ 3 K, a value close to the best values reported [6].

II.   PHEMT MODELLING

As the active element of our amplifier we chose *Agilent ATF35143*, a pseudomorphic AlGaAs/InGaAs/GaAs pHEMT [10]. For this device the gate length is 0.5 μm and the gate width is 400 μm. Other layout details were not given in spite of several requests. We selected this pHEMT due to its excellent reported room temperature noise properties that we expected to improve upon refrigerating the device [9].

The design process was started by measuring the low temperature characteristics of the pHEMT. We soldered it on a printed circuit board attached on to a dip-stick that was immersed into a bath of liquid helium (4.2 K). The scattering parameters were measured using HP 8753 network analyzer. TRL calibration method [11] was used to correct the effect of the signal cables and transitions to the pHEMT. The complex two-port S-parameters were measured on a two-dimensional grid of 8×8 points on plane spanned by measured gate-source (V_{gs}) and drain-source (V_{ds}) voltages. Also bias currents I_{ds} were measured. Using Aplac Software [12], we made a two-dimensional polynomial fit to the data in order to represent the complex S-parameters $S_{ij}(V_{gs}, V_{ds})$ and drain-source current $I_{ds}(V_{gs}, V_{ds})$ as functions of control voltages. The result is illustrated in Fig. 1 as a constant current contour plot. Fig. 2 displays how the gain and drain-source current depend on V_{gs}.

We decided to model the noise parameters of the pHEMT instead of measuring them directly. Bias voltages were selected with reasonable power dissipation, bias current and gain. Small signal model values including package parasitics, as illustrated in Fig. 3, were determined for this DC working point. This was done by fitting the small signal network to the measured complex S-parameters. The measured response compared with the response from small signal model is illustrated in Fig. 4.

Pospiezalski noise model [9] was used for the description of the pHEMT noise characteristics. Noise was included in the small-signal model by assigning effective temperatures to all dissipative elements of the circuit: The gate-source resistance R_{gs} was set to T_{gs}, the channel conductance G_{ch} to T_{ch} and all other resistive elements to bath temperature T_0.

As a confirmation of our small signal model, we fitted our model parameters to the room-temperature noise- and S-parameters taken from manufacturer's data-sheets [10] at $V_{ds} = $ 2 V and $I_{ds} = 5$ mA. We found good agreement with the model when $T_{gs} = T_0 = 349$ K and $T_{ch} = 1941$ K. These values are physically reasonable. T_{ch} is relatively high, presumably due

3

to hot electrons and self-heating effects.

In order to calculate the cryogenic pHEMT noise parameters we made the conservative assumption that $T_{gs} \sim 5$ K and $T_0 \sim 5$ K at $T = 4.2$ K. T_{ch} was assumed to be by a factor 4 lower than its room temperature value. This is a crucial assumption which, however, is in accordance with other similar designs [9, 13] as well as our noise measurement results. The fact that the refrigeration of the pHEMT package does not cool down the channel temperature in proportion can be understood, at least partly, by self-heating effects [14]. This means that even with reasonably low power dissipation (~ 4 mW) the low value of the substrate thermal conductivity builds up a thermal gradient between the channel and the heat bath to which the pHEMT is anchored. Using the temperature estimates above, we generated the 4.2-K S- and noise-parameters that were used in the final amplifier design.

III. AMPLIFIER DESIGN

The design goals for the amplifier were low noise, reasonable gain (> 15 dB) and small return loss ($S_{11} <$ -10 dB). In order to fulfill these conflicting goals, we chose a balanced configuration [15] that gives a reasonable return loss without compromising noise or gain. Fig. 5 illustrates the general scheme of the amplifier that consists of two amplifier blocks and two hybrids splitting the incoming power into two equal parts shifted by 90 degrees in phase with respect to each other. Hybrids were implemented using strip-line Lange couplers [16].

The amplifier block consists of a pHEMT, discrete passive surface mount components and strip-line components as displayed in Fig. 6. The gate-source section is biased by grounding the gate and by lifting the source potential using a resistor as in Ref. [17]. This feedback configuration of a constant drain-source current means that fewer external voltage sources are needed for biasing, the pHEMT is more persistent against static discharge, and there is no direct signal path from the bias leads to the gate electrode. A drawback is that the amplifier can only be tuned by adjusting a single voltage source.

The final design step was to allow all component values to vary within reasonable limits for optimized noise, gain and return loss. The parameter space was considerable, but we were able to find reasonable results by mixing global and local optimization methods and manual tuning.

The frequency range in the modelling was 400–2400 MHz due to the TRL calibration

that was used in our pHEMT characterization at 4.2 K. The amplifier was designed to be unconditionally stable within the modelled frequency range. The amplifier prototype had oscillations at frequencies > 10 GHz, where we had not measured the pHEMT characteristics. After reducing the bias voltage V_{bias} from 1.8 V to 1.45 V the amplifier became stable with both 50 Ω load and open circuit at input. Fig. 7 illustrates the implementation of the amplifier. The amplifier has a SMA connector for the 50 Ω termination of the Lange coupler. This termination is made external to the housing to allow for the option to cool the termination to a lower temperature than the amplifier temperature. This would reduce the noise power wave [18, 19] that the amplifier sends from its input towards the sample.

IV.   MEASUREMENT RESULTS

The scalar two-port characteristics of the amplifier were measured at $T = 4.2$ K by immersing it into liquid Helium. Figure 8 illustrates the measured amplifier frequency response compared with the simulated one. The results are seen to agree to a certain degree with the simulation. The amplifier embodies many hand-soldered surface-mount components and thus there are many possibilities for small variations between the model and the real device.

In order to determine the noise temperature T_N of the amplifier we employed a noise temperature measurement setup shown in Fig. 9. The figure caption lists the parameter values which are used to calculate the confidence interval for the measurement. The system involved a noise diode in conjunction with a variable room-temperature attenuator and a 20 dB low-temperature attenuator to give a variable noise feed to the amplifier input as in Ref. [20]. The amplifier was in vacuum, anchored to a metal plate connected to liquid helium bath. We used two identical amplifiers in cascade to make the contribution of the room temperature amplifier to the measured noise temperature negligible.

Fig. 10a illustrates the relationship between the room-temperature attenuator attenuation α_{RT} and the excess noise T_{ex} at the amplifier input. With the term excess noise we mean the noise contribution at the amplifier input from all other components except from the amplifier. The excess noise is calculated, using formula $T_{out} = T_{in}L + (1 - L)T_{comp}$ separately for each component between the noise diode and the amplifier input. T_{in} describes the input noise that is attenuated by a factor L when it goes through the component at temperature T_{comp}

[21]. T_{out} is the T_{in} for the next component, etc.

For each frequency we measured the noise power over a bandwidth of 5 MHz using an averaging factor of 100. The procedure was repeated for different room temperature attenuator settings corresponding to different values of excess noise at the amplifier input. Attenuator values were varied manually in a such a way that the excess noise displayed an alternating series {50 K, 7.2 K, 40 K, 7.7 K, ... , 13.8 K}. This method reduced the effects of the system gain variation over the measurement time spanning a couple of hours. By using the equation

$$N = G(T_N + T_{ex}) \tag{1}$$

for the measured noise N and excess noise T_{ex}, we fitted a line to find the parameters T_N and G. G is the total gain from amplifier input to the spectrum analyzer with resolution bandwidth of 5 MHz. A linear fit was done for every frequency, for different bias points, and for the system component parameters that give the highest and the lowest T_N. We thus got an array of noise temperatures corresponding to different frequencies and bias voltages. Fig. 10b displays a typical set of measured data with a corresponding fit at an arbitrary frequency and bias point.

Finally, we plot noise temperatures as a function of frequency for the extrema of the amplifier input component values. Fig. 11 depicts the fitted noise temperatures including measurement uncertainties as the grey area. We measured T_N in steps of 10 MHz and the borders of the grey area in Fig. 11 illustrate fourth order polynomials fitted to the data. Scatter between neighboring frequencies was $< \pm 1$ K. Fig 11 also displays the simulated noise temperature at $T_0 = T_g = 5$ K for all other components in the circuit except the channel temperature that was set to a value of $T_{ch} = 500$ K. This value seem to agree with the measurement data.

fully acknowledged.

---

[1] R. Schoelkopf, P. Wahlgren, A. Kozhevnikov, P. Delsing, and D. Prober, Science **280**, 1238 (1998).

[2] R. J. Schoelkopf and M. H. Devoret, Nature (London) **406**, 1039 (2000).

[3] A. Aassime, G. Johansson, G. Wendin, R. Schoelkopf, and P. Delsing, Phys. Rev. Lett **86**, 3376 (2001).

[4] K. K. Likharev, P. IEEE **87**, 606 (1999).

[5] A. Korotkov and M. Paalanen, Appl. Phys. Lett. **74**, 4052 (1999).

[6] R. F. Bradley, Nucl. Phys. B **72**, 137 (1999).

[7] M.-O. André, M. Mück, J. Clarke, J. Gail, and C. Heiden, Appl. Phys. Lett. **75**, 698 (1999).

[8] S. Weinreb, Elect. Div. Internal Report No. 203, NRAO, (1980).

[9] M. Pospiezalski, IEEE T. Microw. Theory **9**, 1340 (1989).

[10] Agilent technologies, ATF35143 Technical Data.

[11] Hewlett packard application note 1287–9.

[12] Aplac Solutions Corporation, 02600 Espoo, Finland.

[13] J.W. Kooi, Technical Report, http://www.submm.caltech.edu/cso/receivers/papers/ballna.pdf.

[14] Y.-F. Wu et al., IEEE Electr. Device L. **17**, 455 (1996).

[15] K. Kurokawa, Bell Syst. Tech. J. **44**, 1675 (1965).

[16] J. Lange, IEEE T. Microw. Theory **MTT-17**, 1150 (1969).

[17] Agilent Technologies, application note 1174.

[18] P. Penfield, IRE Trans. Circ. Theory **CT-9**, 84 (1962).

[19] J. Engberg and T. Larsen, *Noise Theory of Linear and Nonlinear Circuits*, John Wiley, New York, 1995.

[20] J. Fernandez, TMO Progress Report **42-135** (1998).

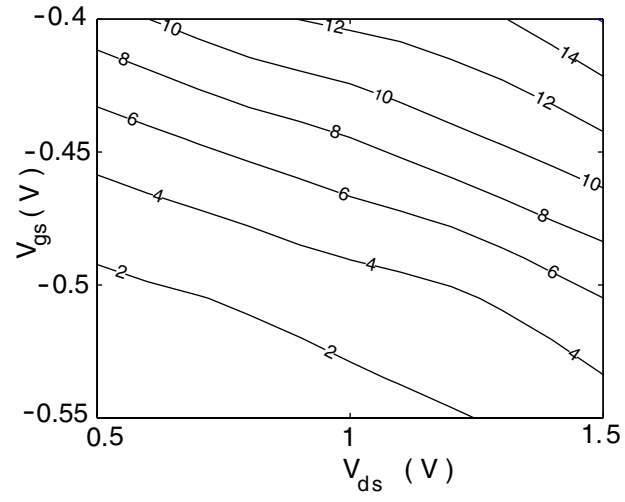[21] D. M. Pozar, *Microwave engineering*, Addison-Wesley, New York, 1st edition, 1990.

FIG. 1: Constant drain-source current I_{ds} contours of the pHEMT at 4.2 K in units of mA as a function of bias voltages.
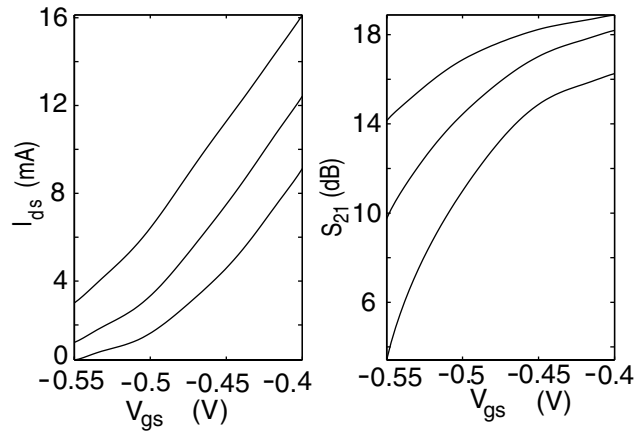
FIG. 2: Drain-source current I_{ds} (a) and gain S_{21}(b) as a function of gate voltage. Three different curves correspond to the drain-source voltages of 0.5, 0.75 and 1 V from bottom to the top, respectively.
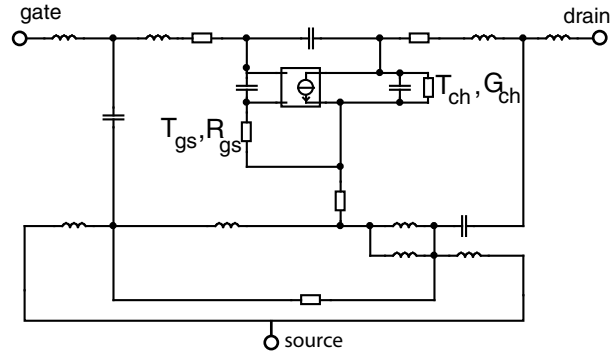
FIG. 3: Small signal model for pHEMT including package parasitics. Network topology is the same as in the data sheet of the manufacturer [10]. T_{gs} and T_{ch} denote the gate and channel temperatures that are used in the noise model.
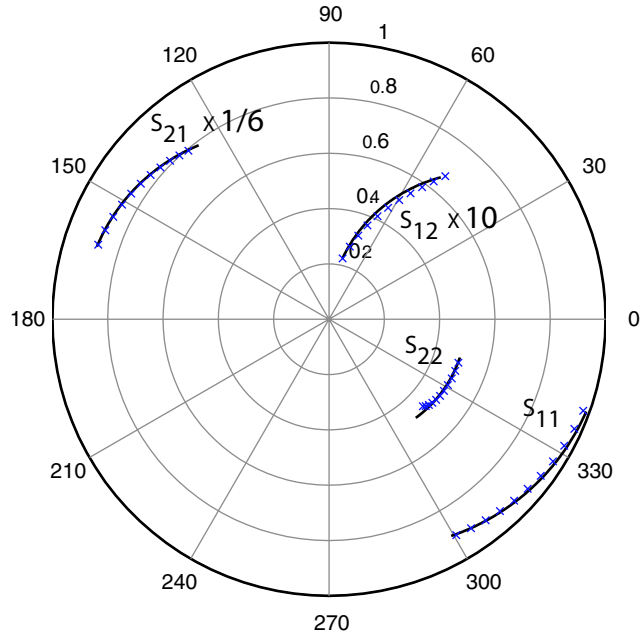
FIG. 4: Comparison between measured pHEMT S-parameters ($\times$) at temperature of 4.2 K and the fitted small-signal model response (line) in polar coordinates. S_{21} is multiplied by factor $1/6$ and S_{12} by factor 10 in the figure. Frequency range is 500 – 1600 MHz.
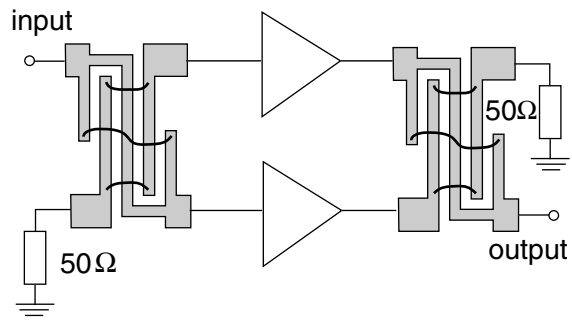
FIG. 5: Schema of the balanced amplifier configuration consisting of two Lange couplers, two 50 Ω terminations and two amplifier blocks that are illustrated in more detail in Fig. 6.
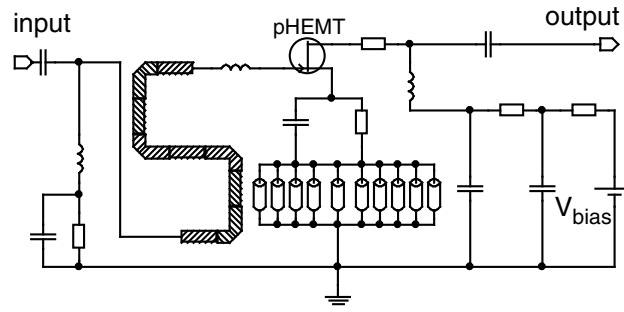
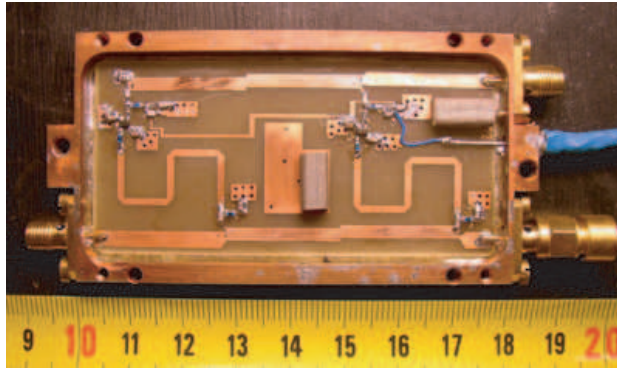FIG. 6: Amplifier block used in the balanced amplifier configuration of Fig. 5.

FIG. 7: Photograph of the amplifier without cover. The amplifier is housed in a high-quality copper enclosure. The coaxial rf-connections are made with SMA -connectors. The scale units at the bottom are centimeters.
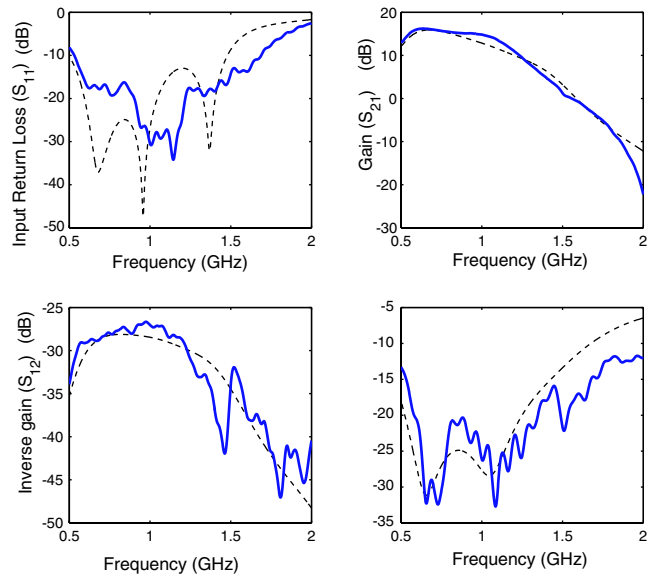
FIG. 8: Simulated (dashed line) and measured (solid line) frequency response of the amplifier at 4.2 K.
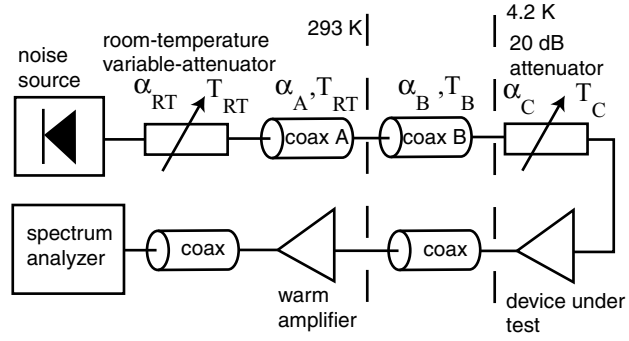
FIG. 9: Schema of the noise calibration setup. The nominal values and the values corresponding to the minimum and maximum noise temperature estimates are the following: Noise source (commercial noise diode) excess noise ratio (ENR) is 13.19 ± 0.1 dB. Variable attenuator attenuation $\alpha_{RT} = 0 \ldots 24 \pm 0.05$ dB. Coaxial cable A: $\alpha_A = 0.3 \pm 0.05$ dB. Coaxial cable B: $\alpha_B = 1.0 \pm 0.2$ dB. Cold attenuator: $\alpha_C = 19.85$ dB ± 1 dB. The effective temperatures for the components are expected to be $T_B = 100$ K (+100 K, –50 K), $T_C = 4.5$ K (+1.5 K, –0.3 K) and $T_{RT} = 293$ K.
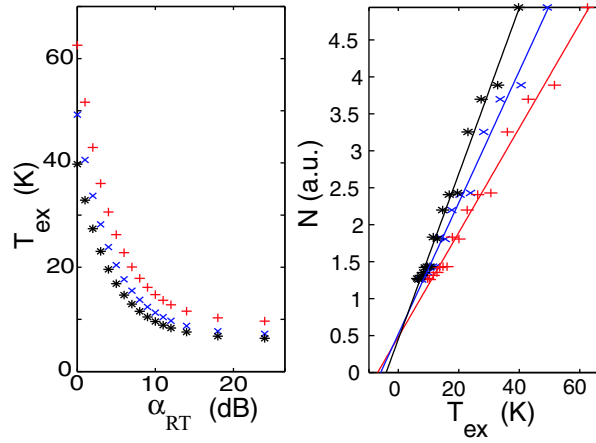
FIG. 10: a) Excess noise T_{ex} at the amplifier input as a function of the room-temperature attenuation α_{RT}. b) Typical measured noise N and a linear fit to extract noise temperature T_N. Symbols denote the expected value ($\times$) and component values giving minimum ($+$) and maximum ($\star$) amplifier noise temperature T_N.
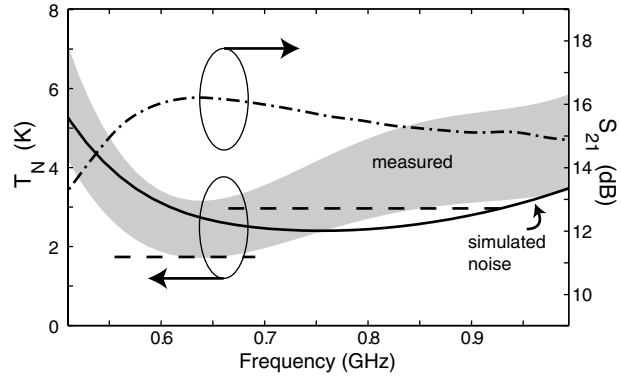
17

FIG. 11: Measured noise temperature T_N with error estimate (gray area) and the result from the simulation (solid line). The dashed lines denote reference noise temperatures of two amplifiers taken from Ref. [6]. Amplifier gain S_{21} is denoted by a dash-dotted line.